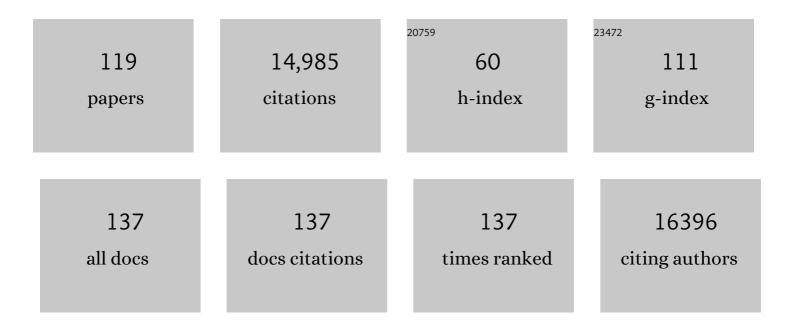
## John A G Briggs

List of Publications by Year in descending order

Source: https://exaly.com/author-pdf/9091675/publications.pdf Version: 2024-02-01



IOHN A C RRICCS

#	Article	IF	CITATIONS
1	Altered TMPRSS2 usage by SARS-CoV-2 Omicron impacts infectivity and fusogenicity. Nature, 2022, 603, 706-714.	13.7	756
2	Cooperative multivalent receptor binding promotes exposure of the SARS-CoV-2 fusion machinery core. Nature Communications, 2022, 13, 1002.	5.8	30
3	Strain and rupture of HIV-1 capsids during uncoating. Proceedings of the National Academy of Sciences of the United States of America, 2022, 119, e2117781119.	3.3	21
4	FCHO controls AP2's initiating role in endocytosis through a PtdIns(4,5)P <sub>2</sub> -dependent switch. Science Advances, 2022, 8, eabn2018.	4.7	14
5	Immature HIV-1 assembles from Gag dimers leaving partial hexamers at lattice edges as potential substrates for proteolytic maturation. Proceedings of the National Academy of Sciences of the United States of America, 2021, 118, .	3.3	40
6	SARS-CoV-2 evolution during treatment of chronic infection. Nature, 2021, 592, 277-282.	13.7	802
7	Structural basis for VPS34 kinase activation by Rab1 and Rab5 on membranes. Nature Communications, 2021, 12, 1564.	5.8	50
8	A stable immature lattice packages IP <sub>6</sub> for HIV capsid maturation. Science Advances, 2021, 7, .	4.7	44
9	Architecture and mechanism of metazoan retromer:SNX3 tubular coat assembly. Science Advances, 2021, 7, .	4.7	44
10	SARS-CoV-2 Spike Protein Stabilized in the Closed State Induces Potent Neutralizing Responses. Journal of Virology, 2021, 95, e0020321.	1.5	35
11	Critical Care Workers Have Lower Seroprevalence of SARS-CoV-2 IgG Compared with Non-patient Facing Staff in First Wave of COVID19. The Journal of Critical Care Medicine, 2021, 7, 199-210.	0.3	4
12	Determining the Patchwork Lattice of Ebola and Marburg Virus Matrix Layers Using Cryo-Electron Tomography. Microscopy and Microanalysis, 2021, 27, 1884-1884.	0.2	0
13	Bridging length-scales from molecules to tissues using mouse genetics, cryoCLEM, and cryoET. Microscopy and Microanalysis, 2021, 27, 2574-2576.	0.2	0
14	Maturation of the matrix and viral membrane of HIV-1. Science, 2021, 373, 700-704.	6.0	60
15	New structural insights into the multifunctional influenza A matrix protein 1. FEBS Letters, 2021, 595, 2535-2543.	1.3	6
16	Structures of virus-like capsids formed by the Drosophila neuronal Arc proteins. Nature Neuroscience, 2020, 23, 172-175.	7.1	46
17	Combined Point-of-Care Nucleic Acid and Antibody Testing for SARS-CoV-2 following Emergence of D614G Spike Variant. Cell Reports Medicine, 2020, 1, 100099.	3.3	61
18	Architecture of the AP2/clathrin coat on the membranes of clathrin-coated vesicles. Science Advances, 2020, 6, eaba8381.	4.7	75

#	Article	IF	CITATIONS
19	A thermostable, closed SARS-CoV-2 spike protein trimer. Nature Structural and Molecular Biology, 2020, 27, 934-941.	3.6	261
20	Complexin Suppresses Spontaneous Exocytosis by Capturing the Membrane-Proximal Regions of VAMP2 and SNAP25. Cell Reports, 2020, 32, 107926.	2.9	33
21	Arrangements of proteins at reconstituted synaptic vesicle fusion sites depend on membrane separation. FEBS Letters, 2020, 594, 3450-3463.	1.3	8
22	The native structure of the assembled matrix protein 1 of influenza A virus. Nature, 2020, 587, 495-498.	13.7	53
23	Structures and distributions of SARS-CoV-2 spike proteins on intact virions. Nature, 2020, 588, 498-502.	13.7	918
24	Structures of immature EIAV Gag lattices reveal a conserved role for IP6 in lentivirus assembly. PLoS Pathogens, 2020, 16, e1008277.	2.1	44
25	Ebola and Marburg virus matrix layers are locally ordered assemblies of VP40 dimers. ELife, 2020, 9, .	2.8	41
26	Structures of immature EIAV Gag lattices reveal a conserved role for IP6 in lentivirus assembly. , 2020, 16, e1008277.		0
27	Structures of immature EIAV Gag lattices reveal a conserved role for IP6 in lentivirus assembly. , 2020, 16, e1008277.		Ο
28	Structures of immature EIAV Gag lattices reveal a conserved role for IP6 in lentivirus assembly. , 2020, 16, e1008277.		0
29	Structures of immature EIAV Gag lattices reveal a conserved role for IP6 in lentivirus assembly. , 2020, 16, e1008277.		0
30	Structures of immature EIAV Gag lattices reveal a conserved role for IP6 in lentivirus assembly. , 2020, 16, e1008277.		0
31	High-throughput ultrastructure screening using electron microscopy and fluorescent barcoding. Journal of Cell Biology, 2019, 218, 2797-2811.	2.3	18
32	Fluorescence-Based Detection of Membrane Fusion State on a Cryo-EM Grid using Correlated Cryo-Fluorescence and Cryo-Electron Microscopy. Microscopy and Microanalysis, 2019, 25, 942-949.	0.2	11
33	Structure of the Ty3/Gypsy retrotransposon capsid and the evolution of retroviruses. Proceedings of the National Academy of Sciences of the United States of America, 2019, 116, 10048-10057.	3.3	39
34	The Neuronal Gene Arc Encodes a Repurposed Retrotransposon Gag Protein that Mediates Intercellular RNA Transfer. Cell, 2018, 172, 275-288.e18.	13.5	382
35	Structure and architecture of immature and mature murine leukemia virus capsids. Proceedings of the National Academy of Sciences of the United States of America, 2018, 115, E11751-E11760.	3.3	92
36	Structure of the membrane-assembled retromer coat determined by cryo-electron tomography. Nature, 2018, 561, 561-564.	13.7	169

#	Article	IF	CITATIONS
37	High-resolution structures of HIV-1 Gag cleavage mutants determine structural switch for virus maturation. Proceedings of the National Academy of Sciences of the United States of America, 2018, 115, E9401-E9410.	3.3	65
38	The contributions of the actin machinery to endocytic membrane bending and vesicle formation. Molecular Biology of the Cell, 2018, 29, 1346-1358.	0.9	52
39	New hardware and workflows for semi-automated correlative cryo-fluorescence and cryo-electron microscopy/tomography. Journal of Structural Biology, 2017, 197, 83-93.	1.3	107
40	Structure of the hexagonal surface layer on Caulobacter crescentus cells. Nature Microbiology, 2017, 2, 17059.	5.9	85
41	Deciphering the Origin and Evolution of Hepatitis B Viruses by Means of a Family of Non-enveloped Fish Viruses. Cell Host and Microbe, 2017, 22, 387-399.e6.	5.1	134
42	Efficient 3D-CTF correction for cryo-electron tomography using NovaCTF improves subtomogram averaging resolution to 3.4 Ã Journal of Structural Biology, 2017, 199, 187-195.	1.3	219
43	Immature HIV-1 lattice assembly dynamics are regulated by scaffolding from nucleic acid and the plasma membrane. Proceedings of the National Academy of Sciences of the United States of America, 2017, 114, E10056-E10065.	3.3	86
44	Structure and assembly of the Ebola virus nucleocapsid. Nature, 2017, 551, 394-397.	13.7	185
45	Implementation of a cryo-electron tomography tilt-scheme optimized for high resolution subtomogram averaging. Journal of Structural Biology, 2017, 197, 191-198.	1.3	556
46	The structure of the COPI coat determined within the cell. ELife, 2017, 6, .	2.8	152
47	9Ã structure of the COPI coat reveals that the Arf1 GTPase occupies two contrasting molecular environments. ELife, 2017, 6, .	2.8	103
48	The structure and flexibility of conical HIV-1 capsids determined within intact virions. Science, 2016, 354, 1434-1437.	6.0	229
49	Higherâ€order assemblies of oligomeric cargo receptor complexes form the membrane scaffold of the Cvt vesicle. EMBO Reports, 2016, 17, 1044-1060.	2.0	26
50	Molecular architecture of the inner ring scaffold of the human nuclear pore complex. Science, 2016, 352, 363-365.	6.0	284
51	Nucleic Acid Binding by Mason-Pfizer Monkey Virus CA Promotes Virus Assembly and Genome Packaging. Journal of Virology, 2016, 90, 4593-4603.	1.5	13
52	An atomic model of HIV-1 capsid-SP1 reveals structures regulating assembly and maturation. Science, 2016, 353, 506-508.	6.0	375
53	Correlative light and electron microscopy methods for the study of virus–cell interactions. FEBS Letters, 2016, 590, 1877-1895.	1.3	71
54	Retrovirus maturation—an extraordinary structural transformation. Current Opinion in Virology, 2016, 18, 27-35.	2.6	64

#	Article	IF	CITATIONS
55	A saposin-lipoprotein nanoparticle system for membrane proteins. Nature Methods, 2016, 13, 345-351.	9.0	209
56	Automated cryo electron tomography and sub-tomogram averaging with the FEI Volta phase plate. Microscopy and Microanalysis, 2015, 21, 1833-1834.	0.2	0
57	A structure of the COPI coat and the role of coat proteins in membrane vesicle assembly. Science, 2015, 349, 195-198.	6.0	159
58	Structural Analysis of the Roles of Influenza A Virus Membrane-Associated Proteins in Assembly and Morphology. Journal of Virology, 2015, 89, 8957-8966.	1.5	78
59	RNA and Nucleocapsid Are Dispensable for Mature HIV-1 Capsid Assembly. Journal of Virology, 2015, 89, 9739-9747.	1.5	17
60	Endocytic sites mature by continuous bending and remodeling of the clathrin coat. Science, 2015, 348, 1369-1372.	6.0	216
61	An Organized Co-assembly of Clathrin Adaptors Is Essential for Endocytosis. Developmental Cell, 2015, 33, 150-162.	3.1	75
62	The Structure of Immature Virus-Like Rous Sarcoma Virus Gag Particles Reveals a Structural Role for the p10 Domain in Assembly. Journal of Virology, 2015, 89, 10294-10302.	1.5	61
63	Structure of the immature HIV-1 capsid in intact virus particles at 8.8ÂÃ resolution. Nature, 2015, 517, 505-508.	13.7	277
64	Insights from reconstitution reactions of COPII vesicle formation using pure components and low mechanical perturbation. Biological Chemistry, 2014, 395, 801-812.	1.2	13
65	The HIV Mutation Browser: A Resource for Human Immunodeficiency Virus Mutagenesis and Polymorphism Data. PLoS Computational Biology, 2014, 10, e1003951.	1.5	25
66	The Nucleocapsid Domain of Gag Is Dispensable for Actin Incorporation into HIV-1 and for Association of Viral Budding Sites with Cortical F-Actin. Journal of Virology, 2014, 88, 7893-7903.	1.5	23
67	Cryo-electron microscopy of tubular arrays of HIV-1 Gag resolves structures essential for immature virus assembly. Proceedings of the National Academy of Sciences of the United States of America, 2014, 111, 8233-8238.	3.3	98
68	Minimal Tags for Rapid Dual olor Live ell Labeling and Superâ€Resolution Microscopy. Angewandte Chemie - International Edition, 2014, 53, 2245-2249.	7.2	254
69	Correlated cryo-fluorescence and cryo-electron microscopy with high spatial precision and improved sensitivity. Ultramicroscopy, 2014, 143, 24-32.	0.8	116
70	Induced Maturation of Human Immunodeficiency Virus. Journal of Virology, 2014, 88, 13722-13731.	1.5	29
71	<scp>SNARE</scp> and regulatory proteins induce local membrane protrusions to prime docked vesicles for fast calciumâ€triggered fusion. EMBO Reports, 2014, 15, 308-314.	2.0	46
72	Schnelle, zweifarbige Proteinmarkierung an lebenden Zellen für die hochauflösende Mikroskopie. Angewandte Chemie, 2014, 126, 2278-2282.	1.6	51

#	Article	IF	CITATIONS
73	Determination of protein structure at 8.5 Ã resolution using cryo-electron tomography and sub-tomogram averaging. Journal of Structural Biology, 2013, 184, 394-400.	1.3	85
74	Structural biology in situ—the potential of subtomogram averaging. Current Opinion in Structural Biology, 2013, 23, 261-267.	2.6	218
75	Variable Internal Flexibility Characterizes the Helical Capsid Formed by Agrobacterium VirE2 Protein on Single-Stranded DNA. Structure, 2013, 21, 1158-1167.	1.6	8
76	Directing Traffic into the Future. Developmental Cell, 2013, 27, 480-484.	3.1	2
77	Vesicle coats: structure, function, and general principles of assembly. Trends in Cell Biology, 2013, 23, 279-288.	3.6	157
78	Tubular endocytosis drives remodelling of the apical surface during epithelial morphogenesis in Drosophila. Nature Communications, 2013, 4, 2244.	5.8	86
79	Nuclear Pore Scaffold Structure Analyzed by Super-Resolution Microscopy and Particle Averaging. Science, 2013, 341, 655-658.	6.0	401
80	The structure of the COPII transport-vesicle coat assembled on membranes. ELife, 2013, 2, e00951.	2.8	112
81	Structural Biology of HIV Assembly. , 2013, , 1-22.		1
82	Imaging cellular structure across scales with correlated light, superresolution, and electron microscopy. Molecular Biology of the Cell, 2012, 23, 979-980.	0.9	5
83	Phosphatidylinositol 4,5-Bisphosphate (PI(4,5)P2)-dependent Oligomerization of Fibroblast Growth Factor 2 (FGF2) Triggers the Formation of a Lipidic Membrane Pore Implicated in Unconventional Secretion. Journal of Biological Chemistry, 2012, 287, 27659-27669.	1.6	96
84	<i>In Vitro</i> Assembly of Virus-Like Particles of a Gammaretrovirus, the Murine Leukemia Virus XMRV. Journal of Virology, 2012, 86, 1297-1306.	1.5	24
85	Complexin arrests a pool of docked vesicles for fast Ca <sup>2+</sup> -dependent release. EMBO Journal, 2012, 31, 3270-3281.	3.5	85
86	Plasma Membrane Reshaping during Endocytosis Is Revealed by Time-Resolved Electron Tomography. Cell, 2012, 150, 508-520.	13.5	320
87	Role of the SP2 Domain and Its Proteolytic Cleavage in HIV-1 Structural Maturation and Infectivity. Journal of Virology, 2012, 86, 13708-13716.	1.5	37
88	The Structures of COPI-Coated Vesicles Reveal Alternate Coatomer Conformations and Interactions. Science, 2012, 336, 1451-1454.	6.0	71
89	Precise, Correlated Fluorescence Microscopy and Electron Tomography of Lowicryl Sections Using Fluorescent Fiducial Markers. Methods in Cell Biology, 2012, 111, 235-257.	0.5	130
90	Structure of the immature retroviral capsid at 8 à resolution by cryo-electron microscopy. Nature, 2012, 487, 385-389.	13.7	152

#	Article	IF	CITATIONS
91	Computational Identification of Novel Amino-Acid Interactions in HIV Gag via Correlated Evolution. PLoS ONE, 2012, 7, e42468.	1.1	7
92	Structural dissection of Ebola virus and its assembly determinants using cryo-electron tomography. Proceedings of the National Academy of Sciences of the United States of America, 2012, 109, 4275-4280.	3.3	210
93	Correlated fluorescence and 3D electron microscopy with high sensitivity and spatial precision. Journal of Cell Biology, 2011, 192, 111-119.	2.3	408
94	The Molecular Architecture of HIV. Journal of Molecular Biology, 2011, 410, 491-500.	2.0	164
95	Multibudded tubules formed by COPII on artificial liposomes. Scientific Reports, 2011, 1, 17.	1.6	86
96	Coatomer and dimeric ADP ribosylation factor 1 promote distinct steps in membrane scission. Journal of Cell Biology, 2011, 194, 765-777.	2.3	70
97	Cryo-Electron Tomography of Marburg Virus Particles and Their Morphogenesis within Infected Cells. PLoS Biology, 2011, 9, e1001196.	2.6	125
98	Virological Synapse-Mediated Spread of Human Immunodeficiency Virus Type 1 between T Cells Is Sensitive to Entry Inhibition. Journal of Virology, 2010, 84, 3516-3527.	1.5	177
99	Conserved and Variable Features of Gag Structure and Arrangement in Immature Retrovirus Particles. Journal of Virology, 2010, 84, 11729-11736.	1.5	52
100	Electron Tomography Reveals the Steps in Filovirus Budding. PLoS Pathogens, 2010, 6, e1000875.	2.1	65
101	Cryo Electron Tomography of Native HIV-1 Budding Sites. PLoS Pathogens, 2010, 6, e1001173.	2.1	119
102	Structural Analysis of HIV-1 Maturation Using Cryo-Electron Tomography. PLoS Pathogens, 2010, 6, e1001215.	2.1	96
103	Computational Model of Membrane Fission Catalyzed by ESCRT-III. PLoS Computational Biology, 2009, 5, e1000575.	1.5	141
104	Contrast transfer function correction applied to cryo-electron tomography and sub-tomogram averaging. Journal of Structural Biology, 2009, 168, 305-312.	1.3	77
105	HIV-1–cellular interactions analyzed by single virus tracing. European Biophysics Journal, 2008, 37, 1291-1301.	1.2	30
106	Three-Dimensional Analysis of Budding Sites and Released Virus Suggests a Revised Model for HIV-1 Morphogenesis. Cell Host and Microbe, 2008, 4, 592-599.	5.1	208
107	Double-labelled HIV-1 particles for study of virus–cell interaction. Virology, 2007, 360, 92-104.	1.1	121
108	Cryo-electron Microscopy Reveals Conserved and Divergent Features of Gag Packing in Immature Particles of Rous Sarcoma Virus and Human Immunodeficiency Virus. Journal of Molecular Biology, 2006, 355, 157-168.	2.0	87

#	ARTICLE	IF	CITATIONS
109	The Mechanism of HIV-1 Core Assembly: Insights from Three-Dimensional Reconstructions of Authentic Virions. Structure, 2006, 14, 15-20.	1.6	188
110	Cryo-Electron Tomographic Structure of an Immunodeficiency Virus Envelope Complex In Situ. PLoS Pathogens, 2006, 2, e83.	2.1	205
111	Classification and three-dimensional reconstruction of unevenly distributed or symmetry mismatched features of icosahedral particles. Journal of Structural Biology, 2005, 150, 332-339.	1.3	34
112	Cryoelectron Microscopy of Mouse Mammary Tumor Virus. Journal of Virology, 2004, 78, 2606-2608.	1.5	21
113	The stoichiometry of Gag protein in HIV-1. Nature Structural and Molecular Biology, 2004, 11, 672-675.	3.6	462
114	Structural organization of authentic, mature HIV-1 virions and cores. EMBO Journal, 2003, 22, 1707-1715.	3.5	390
115	Pathogenic bacteria attach to human fibronectin through a tandem β-zipper. Nature, 2003, 423, 177-181.	13.7	326
116	Do lipid rafts mediate virus assembly and pseudotyping?. Journal of General Virology, 2003, 84, 757-768.	1.3	114
117	Multiple site-specific infrared dichroism of CD3-ζ, a transmembrane helix bundle. Journal of Molecular Biology, 2002, 316, 365-374.	2.0	42
118	Convergence of experimental, computational and evolutionary approaches predicts the presence of a tetrameric form for CD3-ζ. Journal of Molecular Biology, 2002, 316, 375-384.	2.0	35
119	Contribution of Energy Values to the Analysis of Global Searching Molecular Dynamics Simulations of Transmembrane Helical Bundles. Biophysical Journal, 2002, 82, 3063-3071.	0.2	24